PCCP

Ultraviolet photolysis of formyl fluoride: the F + HCO product channel

Christof Maul, Christoph Dietrich,†[a] Tobias Haas,‡[a] Karl-Heinz Gericke,[a] Hiroto Tachikawa,[b] Stephen R. Langford,[c] Mitsuhiko Kono,§[c] Claire L. Reed,¶[c] Richard N. Dixon[c] and Michael N. R. Ashfold*[c]

[a] *Institut für Physikalische und Theoretische Chemie der Technischen Universität Braunschweig, Hans-Sommer-Straße 10, D-38106 Braunschweig, Germany*
[b] *Division of Molecular Chemistry, Graduate School of Engineering, Hokkaido University, Sapporo 060-8628, Japan*
[c] *School of Chemistry, University of Bristol, Bristol UK BS8 1TS.*
E-mail: mike.ashfold@bris.ac.uk

Received 11th December 1998, Accepted 15th January 1999

The time-of-flight spectrum of the H atoms resulting from photodissociation of gas phase HFCO molecules at 243.12 nm indicates a role for secondary photolysis of HCO($\tilde{X}$) fragments arising *via* the F + HCO($\tilde{X}$) dissociation channel. Analysis of this spectrum, and of earlier photofragment translational spectroscopy results obtained at a number of neighbouring wavelengths in the range 218.4–248.2 nm, allow estimation of an upper limit for the C—F bond dissociation energy: D_0(F—CHO) $\leqslant$ 482 kJ mol^{-1}. HCO($\tilde{X}$) fragments are deduced to be amongst the primary products of HFCO photolysis at all wavelengths $\lambda \leqslant 248.2$ nm, indicating that any energy barrier in the F—C bond fission channel [measured relative to the asymptotic products F(^{2}P) + HCO($\tilde{X}$)] must be small. This observation is considered in the light of available knowledge regarding the potential energy surfaces for the ground ($\tilde{X}\,^1A'$) and first excited singlet ($\tilde{A}\,^1A''$) and triplet ($\tilde{a}\,^3A''$) states of HFCO; the available evidence all points to radiationless transfer and subsequent dissociation on the triplet surface as the mechanism for the deduced F—C bond fission.

Introduction

Formyl fluoride, HFCO, is a major degradation product of HFC-134a[1] and, partly for this reason, both its electronic spectroscopy and its photochemistry have been the subject of recent experimental study. The ground ($\tilde{X}\,^1A'$) state of HFCO has a planar equilibrium geometry.[2–4] The $\tilde{A}\,^1A'' \leftarrow \tilde{X}\,^1A'$ absorption system is dominated by a progression in the C=O stretching mode (ν_2), as expected given that the transition involves a $\pi^*_{C=O} \leftarrow n_O$ electron promotion. Giddings and Innes[5] established the band origin of the $\tilde{A} \leftarrow \tilde{X}$ system, ν_0 = 37 491.7 cm^{-1}, the extended CO bond length in the $\tilde{A}$ state, and also deduced the non-planar minimum energy geometry of the $\tilde{A}$ state. However, the barrier to inversion in the $\tilde{A}$ state is too small to preclude tunnelling; the $\tilde{A}$ state is thus legitimately considered as having A″ symmetry under the C_s point group. Assignments of the pattern of $\tilde{A}$ state vibrational levels have since been extended and refined by Fischer[6] and, latterly, by Crane *et al.*[7] using data from jet-cooled laser induced fluorescence (LIF) spectra and *ab initio* calculations.[9]

There are several possible decay processes available to HFCO molecules following excitation to the $\tilde{A}\,^1A''$ state. These include:

$$\text{HFCO}(\tilde{A}) \rightarrow \text{HFCO}(\tilde{X}\,^1A') + h\nu \quad \text{(LIF)} \quad (1)$$

$$\rightarrow \text{HFCO}(\tilde{X}\,^1A') \quad \text{(IC)} \quad (2)$$

$$\rightarrow \text{HFCO}(\tilde{a}\,^3A'') \quad \text{(ISC)} \quad (3)$$

$$\rightarrow \text{H}(^2\text{S}) + \text{FCO}(\tilde{X}\,^2A') \quad (4)$$

$$\rightarrow \text{F}(^2\text{P}) + \text{HCO}(\tilde{X}\,^2A') \quad (5)$$

$$\rightarrow \text{HF(X)} + \text{CO(X)} \quad (6)$$

Amongst the earlier photochemical studies, Klimek and Berry[10] found the HF products resulting from (broadband) UV excitation of HFCO molecules to have an inverted vibrational state population distribution, but that HF vibration still accounted for only ~7% of the available energy. Measurements of the CO formation rate following photoexcitation at 248 and 193 nm led Weiner and Rosenfeld[11] to conclude that the bond fission channels (4) and (5) must be the major dissociation pathways at these wavelengths, with some evidence for the three body dissociation process yielding H + F + CO products at 193 nm. Studies of fragmentation pathway (4) include measurements of the excitation spectrum for forming H atom photofragments following excitation of jet-cooled HFCO molecules (the so-called PHOFEX spectrum),[12,13] analysis of the Doppler lineshapes of these atomic H fragments,[12,13] and high resolution time-of-flight (TOF) measurements of the H atom products resulting from photolysis at many different wavelengths in the range $218.4 \leqslant \lambda \leqslant 248.2$ nm.[14,15] A second, faster, peak in the H

† Present address: Merck KGaA, Frankfurter Str. 250, 64293 Darmstadt, Germany.
‡ Present address: Linopress Publishing Systems GmbH, Frankfurter Str. 21-25, 65760 Eschborn, Germany.
§ Present address: Solar, Terrestrial and Environmental Laboratory and Graduate School of Science, Nagoya University, 3-13, Honohara, Toyokawa 442, Japan.
¶ Present address: Tessella Support Services plc, 3 Vineyard Chambers, Abingdon, UK OX14 3PX.

atom TOF spectra, clearly evident in spectra recorded at $\lambda < 233$ nm, was attributed to secondary photolysis of HCO($\tilde{X}$) fragments,[14,15] thereby reinforcing the earlier suggestion[11] that the F—C bond fission channel (5) contributes to the overall decay of HFCO molecules following excitation to their $\tilde{A}$ state. The H atom PHOFEX spectrum shows well resolved parent rovibronic structure (indicating that the decay is predissociative rather than a direct dissociation), and a clear onset at excitation energies $\sim 39\,690$ cm^{-1} (~ 251.8 nm), considerably above the H—C bond dissociation energy D_0(H—CFO) = 34 950 ± 20 cm^{-1}.[14,15] The difference in these two energies implies the presence of a barrier in the H—CFO exit channel and, clearly, the H atoms observed at the longest excitation wavelengths will arise as a result of H atom tunnelling through this barrier. Photofragment translational spectroscopy (PTS) experiments performed at excitation energies just above this threshold show the FCO($\tilde{X}$) products arising *via* channel (4) to carry only modest rotational excitation, specifically distributed about the *a* inertial axis, with the bulk of the excess energy released as product translation.[15] Excitation at shorter wavelengths results in FCO($\tilde{X}$) products with similar levels of rotational excitation but progressively more vibrational excitation. Modelling the observed excitation wavelength dependence of the energy disposal in the FCO($\tilde{X}$) fragments leads to a best estimate value of $\sim 41\,000$ cm^{-1} for the minimum barrier height in the H—CFO exit channel. All of the experimental observations have been rationalised in terms of a dissociation process initiated by intersystem crossing (ISC) to the $\tilde{a}\,^3A''$ state potential energy surface (PES) and subsequent evolution over (or, by tunnelling, through) an energy barrier to the H + FCO($\tilde{X}$) asymptote.[12–15] *Ab initio* calculations confirm the presence of such an energy barrier on the $\tilde{a}\,^3A''$ state surface.[16,17]

Experimental study of the dissociation of *ground* state HFCO molecules is largely confined to the work of Choi and Moore,[18] who used stimulated emission pumping (SEP) from known $\tilde{A}$ state levels to prepare HFCO($\tilde{X}$) molecules in (known) highly excited rovibrational levels lying below the threshold energies for either of the single bond fission channels (4) and (5). Measurements of the state and energy selected unimolecular decay rate constants thus provide a measure of the threshold energy ($E_a \sim 176$ kJ mol^{-1} or 14 750 cm^{-1}, measured from the $\tilde{X}$ state origin) for dissociation *via* channel (6). The experimental work has been complemented by several theoretical studies of major parts of the $\tilde{X}$ state PES and of the nuclear motions leading to the molecular elimination (6).[19–23]

This paper is particularly concerned with the F—C bond fission channel (5) and extends studies of the H—C fragmentation pathway reported previously by the Bristol group.[12–15] Specifically, we report the H atom velocity distribution resulting from HFCO photolysis at 243.12 nm, and present a re-analysis of earlier higher resolution PTS results obtained at a number of neighbouring wavelengths in the range 218.4–248.2 nm. All provide evidence for HCO($\tilde{X}$) product formation, even at the longest photolysis wavelengths. The analyses provide an upper limit estimate of the F—C bond strength, D_0(F—CHO) $\leqslant$ 482 kJ mol^{-1}, and thus of the enthalpy of formation of the FCO radical, ΔH_f°(FCO). The analyses also lead to the conclusion that any energy barrier in the F—C bond fission channel [measured relative to the asymptotic products F(^{2}P) + HCO($\tilde{X}$)] is small (<1000 cm^{-1}). This observation is considered in the light of available knowledge regarding the PESs for the ground ($\tilde{X}\,^1A'$) and first excited singlet ($\tilde{A}\,^1A''$) and triplet ($\tilde{a}\,^3A''$) states of HFCO. The balance of evidence, reinforced by new *ab initio* data presented here for the minimum energy pathway leading to F—C bond fission on the $\tilde{a}\,^3A''$ state PES, indicates that the deduced F + HCO($\tilde{X}$) products arise as a result of radiationless transfer to, and subsequent dissociation on, this triplet PES.

Experimental

The H atom PTS experiments in Braunschweig and in Bristol have both been described previously. Both involve use of a supersonic molecular beam of the formyl fluoride, which was generated in both laboratories by the reaction between cyanuric fluoride and formic acid[24] and introduced as a molecular beam by passing ~1 atm of Ar over a sample of liquid HFCO stored at dry ice temperature. The former used focused 243.12 nm radiation to effect multiphoton ionisation (resonance enhanced at the two photon energy by the $2s^1$; $^2S_{1/2}$ state) of the H atom fragments. The H atom recoil velocities are determined by measurement of their times-of-flight (TOFs) to a pair of microchannel plates located at the end of a carefully designed TOF spectrometer comprising one acceleration stage followed by a field free drift region.[25] The present experiments involved a single excimer pumped frequency doubled dye laser system to provide the necessary photolysis and REMPI probe wavelengths. Typical pulse energies used were ~0.2 mJ, focused into the interaction volume with a 8 cm f.l. lens. Space charge effects were investigated by systematically varying both the laser pulse energy and the seeding density in the molecular beam, thereby ensuring that the measurements reported here were made under distortion-free conditions. The Bristol experiment employs one Nd–YAG pumped frequency doubled or tripled dye laser to induce photolysis (typical pulse energies 0.5–1.0 mJ, focused using a 50 cm f.l. lens), and a second Nd–YAG laser pumping two dye lasers producing light at $\lambda_1 = 364.6$ nm and $\lambda_2 = 366$ nm. The former radiation is frequency tripled in Kr to generate light at the Lyman-α wavelength which, together with a λ_2 photon, is used to excite the H atom fragments to a high ($n \sim 80$) Rydberg state.[15,26,27] Rydberg atoms that recoil along a flight tube aligned along the direction othogonal to the plane defined by the axes of the molecular beam and the laser beams are field ionised immediately prior to striking a detector placed 425.6 mm from the laser interaction region, thereby yielding a TOF spectrum. Energy and momentum conservation enable this spectrum to be converted into a spectrum of the total kinetic energy release (TKER).

Calculations

Ab initio MO calculations were performed in Hokkaido using the GAUSSIAN 94 package (Revision D.3).[28] The equilibrium structures for the $\tilde{X}\,^1A'$, $\tilde{A}\,^1A''$ and $\tilde{a}\,^3A''$ states of HFCO, and the geometries of the respective transition states leading to F—CHO and H—CFO dissociation on the $\tilde{a}\,^3A''$ state PES were obtained at the MP4SDQ/6-311G(d,p) level. Energy optimisation at these critical geometries was at the MP4SDQ level, using 6-311++G(d,p) and 6-311++G(2d,p) basis sets.

Results and discussion

Fig. 1 shows an H atom TOF spectrum obtained in Braunschweig following 243.12 nm (41 130 cm^{-1}) photolysis of jet-cooled HFCO molecules using linearly polarised light with the electric field vector aligned perpendicular to the TOF axis. The clear maximum at TOF ~51 μs is due to H atoms arising from the primary photolysis step (4), and implies a TKER whose peak and energy width are wholly compatible with the earlier higher resolution PTS studies.[15] The present study is focused on the faster pedestal in the TOF spectrum, the onset of which occurs at TOF ~19.3 μs. The relative importance of this early time pedestal increases with increasing laser pulse energy. This observation, and the fact that the fastest H atoms correspond to a TKER ~35 900 cm^{-1}, are both suggestive of a process involving the absorption of more than one photolysis photon. The parent 'action' spectrum for forming H atoms

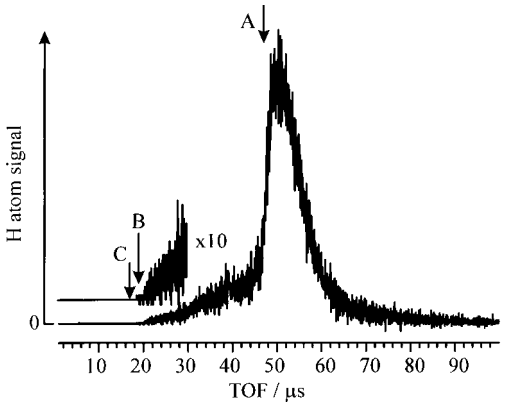

Fig. 1 TOF drift spectrum of H ions generated in HFCO photodissociation/ionisation at 243.12 nm. The major peak at TOF ~51 μs is due to H atoms arising *via* the H—C bond fission channel (4) while the pedestal appearing at earlier times is attributed to secondary photolysis of HCO($\tilde{X}$) fragments arising *via* the F—C bond fission (5). The vertical arrows labelled A, B and C indicate the minimum H atom TOFs expected at this excitation wavelength for the cases of, respectively, one photon dissociation of parent HFCO molecules, one photon dissociation of $HCO(\tilde{X})_{v=0}$ fragments, and two photon dissociation of the parent HFCO.

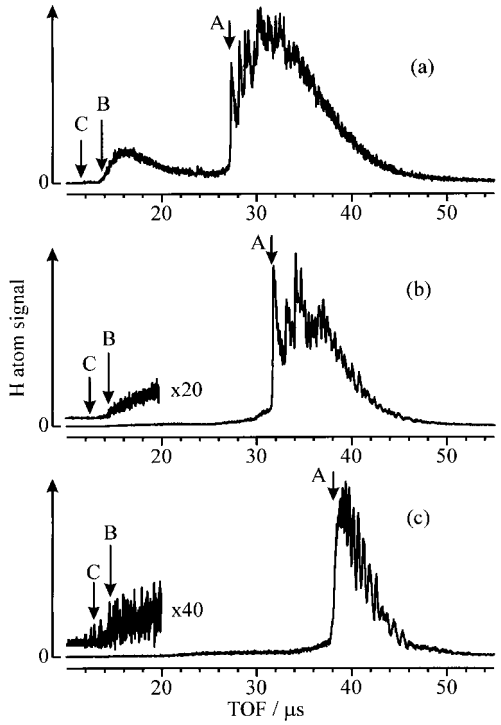

Fig. 2 H (Rydberg) atom TOF spectra obtained following linearly polarised photolysis of a jet-cooled sample of HFCO molecules at (a) 220.0, (b) 234.1 and (c) 248.2 nm. The major peak at later times and the early time pedestal are assigned as in Fig. 1.

shows resolved rovibronic structure[13] indicating that, even this far above its electronic origin, the $\tilde{A}$ state of HFCO has a finite (~ps) lifetime with respect to fragmentation. Thus one possible explanation for such fast H atoms in the TOF spectrum could be two photon excitation of HFCO, resonance enhanced at the one photon energy, and subsequent dissociation to yield H + FCO($\tilde{X}$) fragments with a broad spread of internal energies. An alternative two photon process, involving the one photon dissociation (5) and subsequent one photon excitation and fragmentation of the resulting HCO($\tilde{X}$) fragments was inferred in the earlier PTS study of H atoms arising in the UV photolysis of HFCO, but only at excitation wavelengths shorter than ~233 nm.[15] The vertical arrows labelled A, B and C in Fig. 1 indicate the minimum TOFs compatible with, respectively, one photon absorption by HFCO and subsequent dissociation to H + FCO($\tilde{X}$) fragments, one photon dissociation of $HCO(\tilde{X})_{v=0}$ fragments produced *via* the alternative F—C bond fission channel (5), and with two photon dissociation of HFCO to H + FCO($\tilde{X}$) products. Clearly, this data suggests that such a two step photolysis (B) is operative at longer excitation wavelengths than hitherto recognised, and has encouraged a reappraisal of the earlier data.

Fig. 2 shows H atom TOF spectra taken in Bristol at 220.0, 234.1 and 248.2 nm with, in each case, the polarisation vector of the photolysis laser aligned perpendicular to the TOF axis. The faster H atom signal in Figs. 2(b) and (c) is less evident than that in Fig. 1, reflecting the lower laser intensities used in the Bristol work. Nonetheless, it is clear that the relative showing of the fast signal declines as the photolysis wavelength is increased. In each case the onset at short TOF is seen to match better with interpretation B, and reinforces the idea that primary F—C bond fission occurs at excitation wavelengths as long as 248.2 nm. The difference in thresholds B and C look deceptively small when plotted on a TOF scale but actually correspond to a TKER difference of $[h\nu - D_0(\text{H—CFO}) + D_0(\text{H—CO})]$ which, at 234.1 nm, for example, is ~13000 cm^{-1}. We also caution against reading much into the relative intensities of the slower (primary photolysis) and faster pedestal (secondary photolysis) contributions to these H atom TOF spectra. The $\tilde{B}$–$\tilde{X}$ and $\tilde{C}$–$\tilde{X}$ systems of HCO have origins at 38691 and 41270 cm^{-1}, respectively,[29] and given the geometry changes that accompany these electronic excitations, we can anticipate that this radical will absorb throughout the wavelength range of interest. However, the HCO absorption cross-section at any particular wavelength can be expected to depend sensitively upon the internal state population distribution within the HCO($\tilde{X}$) fragments; this in turn will be a reflection of the dissociation dynamics of channel (5) and is likely to be excitation wavelength dependent. Further, of course, as we have commented previously, the relative showing of these two contributions to the H atom TOF spectrum exhibit different laser power dependencies. Thus, while we feel confident about interpreting the observed pedestal in the TOF spectra as indicating a contribution from the F—C bond fission channel (5), we are unable to comment on relative quantum yields. We note that very analogous secondary photolysis of HCO($\tilde{X}$) radicals has been observed in the photolysis of the isoelectronic molecule HCOOH in this same wavelength range.[30]

Thermochemistry: D_0(F—CHO) and $\Delta H_{f,0}°$(FCO)

Given $D_0(\text{H—CFO}) = 34950 \pm 20$ cm^{-1} (418.0 ± 0.2 kJ mol^{-1}) and the established value for $\Delta H_{f,0}°(\text{H})$[31] (see Table 1), $\Delta H_{f,0}°$(HFCO) can be calculated from eqn. (7) if $\Delta H_{f,0}°$(FCO) is known;

$$\Delta H_{f,0}°(\text{HFCO}) = \Delta H_{f,0}°(\text{H}) + \Delta H_{f,0}°(\text{FCO}) - D_0(\text{H—CFO}) \quad (7)$$

Unfortunately, as Table 1 also shows, considerable uncertainty is still attached to this last enthalpy of formation. Two

Table 1 Enthalpies of formation used in the estimation of D_0(F—CHO)

Species	$\Delta H_{f,0}°$/kJ mol^{-1} (ref.)
H	216.04 (31)
F	77.3 (31)
FCO	-153 ± 12 (32); -161 ± 8 (33) -183 ± 7 (34); -184.5 ± 2 (35)
HCO	44.0 ± 0.4 (36); 41.5 ± 0.8 (37)

recent experimental studies[32,33] yield values of $\Delta H_{f,0}^{o}(FCO) = -153 \pm 12$ and -161 ± 8 kJ mol^{-1}, respectively, which imply $\Delta H_{f,0}^{o}(HFCO) \sim -359 \pm 12$ kJ mol^{-1}. Worryingly, however, contemporary high level *ab initio* calculations[34,35] suggest the substantially more negative values for $\Delta H_{f,0}^{o}(FCO)$ shown in Table 1, thereby implying $\Delta H_{f,0}^{o}(HFCO) \sim -387 \pm 3$ kJ mol^{-1}. The discrepancy in these two sets of values for $\Delta H_{f,0}^{o}(HFCO)$ will map directly into any estimation of the F—C bond strength, D_0(F—CHO):

$$D_0(F—CHO) = \Delta H_{f,0}^{o}(F) + \Delta H_{f,0}^{o}(HCO) - \Delta H_{f,0}^{o}(HFCO) \quad (8)$$

$\Delta H_{f,0}^{o}(F)$ is well established[31] but, to complicate matters further, there is also some uncertainty regarding the enthalpy for forming HCO radicals. As Table 1 illustrates, the most recent assessment, $\Delta H_{f,0}^{o}(HCO) = 44.0 \pm 0.4$ kJ mol^{-1},[36] fails to encompass what hitherto had been considered the most accurate value deduced from measurements of the threshold energies for forming H(D) atoms in the tunable UV photolysis of $H_2CO(D_2CO)$.[37] However, these discrepancies are small compared with the uncertainty attached to $\Delta H_{f,0}^{o}(FCO)$. Adopting the more recent value of $\Delta H_{f,0}^{o}(HCO)$[36] we arrive at the following estimates of the F—C bond strength: $D_0(F—CHO) = 480 \pm 12$ kJ mol^{-1} ($40\,100 \pm 1000$ cm^{-1}) if we take the mean of the recent experimental determinations of $\Delta H_{f,0}^{o}(FCO)$ (-157 ± 12 kJ mol^{-1}); or $D_0(F—CHO) = 508 \pm 2$ kJ mol^{-1}($42\,500 \pm 250$ cm^{-1}) if $\Delta H_{f,0}^{o}(FCO) = -184.5 \pm 2$ kJ mol^{-1}. Both values are higher than that erroneously suggested in earlier PTS studies of the H atoms resulting from UV photolysis of HFCO.[14,15]

Extracting a value for D_0(F—CHO) from the present experiments is complicated by uncertainties regarding (a) the contribution that parent hot band absorption may be making to the deduced F + HCO($\tilde{X}$) yield observed at the longest excitation wavelengths and (b) the internal energy state of the HCO($\tilde{X}$) fragments undergoing secondary photolysis. For example, if we attribute the fastest H atoms observed at $\lambda = 248.2$ nm to secondary photolysis of $HCO(\tilde{X})_{v=0}$ fragments then we obtain $D_0(F—CHO) \leqslant 482$ kJ mol^{-1}, and lower limit estimates for $\Delta H_{f,0}^{o}(HFCO) \geqslant -361$ kJ mol^{-1} and $\Delta H_{f,0}^{o}(FCO) \geqslant -159$ kJ mol^{-1}, in good accord with other recent experimental determinations.[32,33] This good agreement, in turn, suggests that any energy barrier in the F—CHO exit channel must be small. These findings raise further questions regarding the recent theoretical estimates for $\Delta H_{f,0}^{o}(FCO)$ (-184.5 ± 2 kJ mol^{-1}),[34,35] which imply a value of $\sim$235 nm for the long wavelength threshold for F + HCO($\tilde{X}$) production. Such a value can only be reconciled with the present experimental findings by assuming exceptionally (improbably?) favourable Franck–Condon factors for exciting the very small fraction of parent molecules in the molecular beam carrying sufficient internal excitation ($\sim$2200 cm^{-1} in the case of $\lambda = 248.2$ nm) to exceed the threshold energy for channel (5).

HFCO fragmentation dynamics

Interpreting the fast component of the H atom TOF signal as evidence for primary F—C bond fission at excitation wavelengths as long as 248.2 nm necessitates some reconsideration of the fragmentation dynamics of HFCO. The structured appearance of the parent absorption spectrum at these wavelengths is taken as evidence that the fragmentation is predissociative. This is in accordance with expectations based on symmetry considerations,[15] which show the $\tilde{X}$ state of HFCO to correlate with the ground state H—C bond fission products, H + FCO($\tilde{X}\,^2A'$), while the parent $\tilde{A}$ state correlates adiabatically with the lowest energy excited products of A″ symmetry. *Ab initio* calculations[38,39] suggest that the threshold for this H + FCO($1\,^2A''$) product channel is $\sim$25 000 cm^{-1} above the ground state asymptote.

Two possible routes to the ground state FCO($\tilde{X}$) products identified following photo-excitation to the $\tilde{A}$ state of HFCO can be envisaged.[12–15] Crane *et al.*[7] have clearly shown the importance of internal conversion (IC) to the ground state surface at excitation energies *below* the threshold for the H + FCO($\tilde{X}$) radical channel, and concurrent studies from Choi and Moore indicate that molecular elimination to the products HF + CO is dominant at these energies.[18] We have argued previously, however, that IC is unlikely to provide the route for $\tilde{A}$ state parent molecules to dissociate to ground state radical products (4), since analyses of the H atom Doppler lineshapes[12,13] and the PTS experiments[14,15] both provide unequivocal evidence for the presence of an energy barrier (of $\sim$5000 cm^{-1} measured relative to the asymptotic products) in the exit channel leading to H + FCO($\tilde{X}$) products. Neither correlation arguments nor *ab initio* calculations[9,16] suggest any significant barrier in the H—C dissociation co-ordinate of the $\tilde{X}$ state surface. ISC to the $\tilde{a}\,^3A''$ surface is an alternative fragmentation route by which $\tilde{A}$ state HFCO molecules could evolve to ground state H + FCO products, and all recent studies suggest that this is the initial step in the radical dissociation channel (4). The observed exit channel barrier is explicable since the triplet surface supports the bottom half of a conical intersection. The magnitude of the associated energy barrier decreases with increasing out of plane bending angle, but is calculated[16,17] still to be very significant at the transition state to fragmentation *via* H—C bond fission.

Information on the alternative radical dissociation channel (5) is more sparse. Direct dissociation on the $\tilde{A}$ state surface is unlikely, given the finite excited state lifetime at the excitation energies relevant to this study. Early *ab initio* calculations[16] hinted at a large barrier to F—C bond fission on the $\tilde{a}$ state PES. If correct, this would rule out dissociation after ISC as a route to the deduced F + HCO($\tilde{X}$) product formation following photoexcitation at the longer wavelengths used in this work. By default therefore, it would be necessary to propose IC and subsequent dissociation on the ground state surface as the route for forming these products. Such an explanation would be compatible with the present finding that there is little or no energy barrier in the exit channel leading to F + HCO($\tilde{X}$) products, but is not without its problems. Principal amongst these is the fact that the dissociation asymptote for forming H + FCO($\tilde{X}$) products lies below that for F + HCO($\tilde{X}$) product formation. The current consensus view is that neither of these exit channels *on the ground state surface* involves passage over or through an activation barrier. That being the case, any statistical fragmentation model would suggest that at any given energy the rate of H—C bond fission must dominate that of F—C bond fission, and that neither product channel will be as significant as the molecular elimination (6). Yet the observed fast H atoms are attributed to secondary photolysis of HCO($\tilde{X}$) products, *i.e.* secondary photolysis (which must be a relatively inefficient process under the prevailing experimental conditions) of a product of what, seemingly, is the least likely fragmentation process available to HFCO($\tilde{X}$) molecules.

This suggests one of two things. Either, direct H atom loss on the $\tilde{X}$ state surface [channel (4)] is much less facile (relative to F atom loss) than simple statistical considerations might suggest, or that we should look again at the initial assumption that the deduced F—C bond fission process must occur on the $\tilde{X}$ state PES. The former suggestion could be accommodated if, for example, the initial nuclear motions leading towards H—C bond fission on the ground state surface involve passage through a region of phase space where H atom capture by the F atom and subsequent elimination of HF was

Table 2 Optimised geometries, harmonic frequencies and zero-point energies (E_z) of HFCO molecules at the minima of the $\tilde{X}\,^1A'$ and $\tilde{a}\,^3A''$ state PESs and at the transition states leading to H—C and F—C bond fission on the $\tilde{a}$ state surface (TS4 and TS5, respectively), calculated at the MP4SDQ/6-311G(d,p) level of theory

	$\tilde{X}\,^1A'$	$\tilde{a}\,^3A''$	TS4	TS5
r(C—O)/Å	1.1809	1.3497	1.2019	1.2095
r(C—F)/Å	1.3423	1.3443	1.3405	1.7797
r(C—H)/Å	1.0953	1.0963	1.5248	1.1101
< OCF/degrees	123.08	111.64	126.46	91.27
< OCH/degrees	127.71	111.19	92.62	123.01
< H—COF/degrees (dihedral angle)	180.0	128.18	104.58	97.67
ν_1/cm^{-1}	3160.0	3099.3	2152.4i	2896.2
ν_2/cm^{-1}	1915.0	1380.4	1806.9	1080.3i
ν_3/cm^{-1}	1432.5	1180.4	1055.7	1661.1
ν_4/cm^{-1}	1113.0	1146.4	841.7	1129.6
ν_5/cm^{-1}	1078.3	1035.8	717.3	764.4
ν_6/cm^{-1}	686.4	508.0	553.6	291.8
E_z/cm^{-1}	4692.2	4175.2	2487.6	3371.6
E_z/kJ mol^{-1}	56.1	59.8	29.8	40.3

the norm. This seems unlikely to be sufficiently efficient to suppress all H—C bond fission.

The alternative explanation requires that F—C bond cleavage, like the observed H—C bond fission, in fact occurs on the triplet PES, after ISC from the initially populated $\tilde{A}$ state. This would run counter to the findings of the early theoretical calculations of the topology of the $\tilde{a}\,^3A''$ state PES,[16] but is not precluded by symmetry considerations since the F(^{2}P) + HCO($\tilde{X}$) combination can correlate with one singlet and one triplet parent state of A″ symmetry (and two of each multiplicity of A′ symmetry). This prompted a theoretical reinvestigation, in Hokkaido, of the minimum energy pathway to F—C bond fission on the $\tilde{a}\,^3A''$ state surface. Tables 2 and 3 show, respectively, the optimised geometries, harmonic frequencies and zero-point energies at the minima of the $\tilde{X}$ and $\tilde{a}$ state PESs, and at the transition states (the minimum energy barriers) leading to H—C (TS4) and F—C (TS5) bond fission on the $\tilde{a}\,^3A''$ state surface. The calculations reproduce well the experimentally determined minimum energy geometry of the $\tilde{X}$ state, and slightly underestimate the energy barrier associated with TS4 (measured relative to the asymptotic products). Most importantly, they reveal that the barrier to F—C bond fission on the $\tilde{a}\,^3A''$ state surface (TS2) is much smaller than implied by the earlier lower level calculations,[16] which employed a tight basis set (6-31G*) and in which electron correlation was treated at the MP2 level only. These results lend strong support to the proposal that the deduced F—C bond fission does indeed occur on the $\tilde{a}\,^3A''$ state surface. Such an explanation is also consistent with the deduced efficiency of dissociation process (5) and, if neither bond fission process was competitive with molecular elimination on the $\tilde{X}$ state PES, would accord with the non-observation of primary H atom products at excitation energies below ~39 690 cm^{-1}, *i.e.* below the minimum energy for H atom tunnelling through the barrier to H—C bond fission on the $\tilde{a}\,^3A''$ state surface. Fig. 3 provides a schematic diagram illustrating the relative energetics of these competing bond fission channels.

Table 3 Total electronic energies (E_h) at the minima of the $\tilde{X}$ and $\tilde{a}$ state PESs, and at the configurations corresponding to the minimum energy barriers leading to H—C and F—C bond fission on the $\tilde{a}$ state surface (TS4 and TS5, respectively), calculated at three different levels of theory, for structures that have been fully optimised at the MP4SDQ/6-311G(d,p) level (Table 2). Also shown are the calculated $\tilde{a}$–$\tilde{X}$ state energy separation (without, ΔE, and with, ΔE_z, inclusion of the respective zero-point energies) and the energies of the activation barriers to H—C and F—C bond fission, measured relative to the $\tilde{a}$ state minimum (again without, E_a, and with, E'_a inclusion of the change in respective zero-point energies), in kJ mol^{-1} (and, in parentheses, in cm^{-1})

	MP4SDQ /6-311G(d,p)	MP4SDQ /6-311++G(d,p)	MP4SDQ /6-311++G(2d,p)
$\tilde{X}\,^1A'$	−213.34844	−213.35881	−213.40309
$\tilde{a}\,^3A''$	−213.19257	−213.20383	−213.24741
TS4	−213.14960	−213.15990	−213.20447
TS5	−213.14196	−213.15402	−213.19806
ΔE($\tilde{a}$–$\tilde{X}$)	409.2 (34 210)	406.9 (34 015)	408.7 (34 167)
ΔE_z($\tilde{a}$–$\tilde{X}$)	6.3 (517)		
E_a(TS4)	113.0 (9945)	115.5 (9655)	112.5 (9411)
E_a(TS5)	133.1 (11 125)	131.0 (10 950)	129.7 (10 845)
E'_a(TS4)	92.9 (7766)	95.1 (7959)	92.5 (7731)
E'_a(TS5)	123.4 (10 320)	121.3 (10 145)	120.1 (10 040)

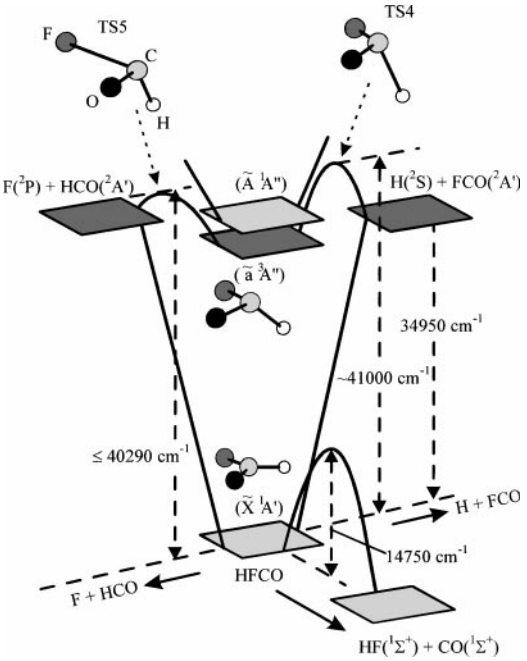

Fig. 3 Schematic energy level diagram illustrating the various parent → product correlations considered in this work, and the location and nuclear configurations at the $\tilde{X}$ and $\tilde{a}$ state potential minima and at the transition states leading to H—C and F—C bond fission on the $\tilde{a}$ state PES. Channel (4) is observed to open at excitation energies ~39 690 cm^{-1}, as a result of tunnelling through the barrier in the H—C dissociation coordinate.

Conclusions

Arguments presented in this work suggest that processes (1)–(6) all contribute to the decay of an ensemble of $\tilde{A}$ state HFCO molecules. H—C bond fission (4) is a significant loss process following excitation at energies above ~39 690 cm^{-1}; it occurs after ISC to the $\tilde{a}\,^3A''$ PES and involves passage over (or, near threshold, through) an exit channel barrier of energy ~5000 cm^{-1} (measured relative to the asymptotic products). The present work suggests that the alternative F—C bond cleavage (5) also occurs as a result of ISC to the $\tilde{a}\,^3A''$ state PES, that it makes some contribution at all wavelengths $\lambda \leqslant 248.2$ nm, and that it involves minimal activation barrier. ISC is considered to be the dominant non-radiative decay route for HFCO($\tilde{A}$) molecules following excitation to energies above these bond fission thresholds; the available experimental evidence, and statistical considerations, indicate that the molecular elimination channel (6) is the dominant decay route for that fraction of the excited HFCO molecules that undergo IC to the ground state.

Acknowledgements

The Bristol group are grateful to the EPSRC and NERC for financial support, and to K. N. Rosser and P. A. Cook for help, advice and encouragement. M. K. thanks the Japanese Society for the Promotion of Science for the award of a Postdoctoral Research Fellowship. The Braunschweig group gratefully acknowledges R. J. Gdanitz for fruitful discussions and the Deutsche Forschungsgemeinschaft for financial support.

References

1 T. J. Wallington, M. D. Hurley, J. C. Ball and E. W. Kaiser, *Environ. Sci. Technol.*, 1992, **26**, 1318.
2 H. W. Morgan, P. A. Staats and J. H. Goldstein, *J. Chem. Phys.*, 1955, **25**, 337.
3 P. Favero, A. M. Mirri and J. G. Baker, *J. Chem. Phys.*, 1956, **31**, 566.
4 O. LeBlanc, Jr., W. W. Laurie and W. D. Gwinn, *J. Chem. Phys.*, 1960, **33**, 1960.
5 L. E. Giddings, Jr. and K. K. Innes, *J. Mol. Spectrosc.*, 1961, **6**, 528; 1962, **8**, 328.
6 G. Fischer, *J. Mol. Spectrosc.*, 1969, **29**, 37.
7 J. C. Crane, H. Nam, H. P. Beal, H. Clauberg, Y. S. Choi, C. B. Moore and J. F. Stanton, *J. Mol. Spectrosc.*, 1997, **181**, 56.
8 Y. S. Choi, PhD Thesis, U. C. Berkeley, 1991.
9 J. F. Stanton and J. Gauss, *Theor. Chim. Acta*, 1995, **91**, 267.
10 D. E. Klimek and M. J. Berry, *Chem. Phys. Lett.*, 1973, **20**, 141.
11 B. R. Weiner and R. N. Rosenfeld, *J. Phys. Chem.*, 1988, **92**, 4640.
12 R. N. Dixon and T. W. R. Hancock, *J. Phys. Chem. A*, 1997, **101**, 7567.
13 T. W. R. Hancock and R. N. Dixon, *J. Chem. Soc., Faraday Trans.*, 1997, **93**, 2707.
14 C. L. Reed, M. Kono, S. R. Langford, T. W. R. Hancock, R. N. Dixon and M. N. R. Ashfold, *J. Chem. Phys.*, 1997, **106**, 6198.
15 C. L. Reed, M. Kono, S. R. Langford, R. N. Dixon and M. N. R. Ashfold, *J. Chem. Soc., Faraday Trans.*, 1997, **93**, 2721.
16 R. Sumathi and A. K. Chandra, *Chem. Phys.*, 1992, **165**, 257.
17 H. Tachikawa, Hokkaido University, unpublished results reported in ref. 15.
18 Y. S. Choi and C. B. Moore, *J. Chem. Phys.*, 1991, **94**, 5414; 1992, **97**, 1010; 1995, **103**, 9981.
19 K. Kamiya and K. Morokuma, *J. Chem. Phys.*, 1991, **94**, 7287.
20 J. S. Francisco and Y. Zhao, *J. Chem. Phys.*, 1992, **96**, 7587.
21 T-G. Wei and R. E. Wyatt, *J. Phys. Chem.*, 1993, **97**, 13580.
22 T. Yamamoto and S. Kato, *J. Chem. Phys.*, 1997, **107**, 6114; 1998, **109**, 9783.
23 F. E. Budenholzer and T. Yu, *J. Phys. Chem. A*, 1998, **102**, 947.
24 G. A. Olah, M. Nojima and I. Kerekes, *Synthesis*, 1973, 487.
25 T. Haas, K-H. Gericke, C. Maul and F. J. Comes, *Chem. Phys. Lett.*, 1993, **202**, 108.
26 L. Schnieder, W. Meier, K. H. Welge, M. N. R. Ashfold and C. M. Western, *J. Chem. Phys.*, 1990, **92**, 7027.
27 M. N. R. Ashfold, D. H. Mordaunt and S. H. S. Wilson, *Adv. Photochem.*, 1996, **21**, 217.
28 M. J. Frisch, G. W. Trucks, H. B. Schlegel, P. M. W. Gill, B. G. Johnson, M. A. Robb, J. R. Cheeseman, T. Keith, G. A. Petersson, J. A. Montgomery, K. Raghavachari, M. A. Al-Laham, V. G. Zakrzewski, J. V. Ortiz, J. B. Foresman, J. Cioslowski, B. B. Stefanov, A. Nanayakkara, M. Challacombe, C. Y. Peng, P. Y. Ayala, W. Chen, M. W. Wong, J. L. Andres, E. S. Replogle, R. Gomperts, R. L. Martin, D. J. Fox, J. S. Binkley, D. J. Defrees, J. Baker, J. P. Stewart, M. Head-Gordon, C. Gonzalez and J. A. Pople, Gaussian, Inc., Pittsburgh, PA, 1995.
29 R. N. Dixon, *Trans. Faraday Soc.*, 1969, **65**, 3141.
30 S. R. Langford, A. D. Batten, M. Kono and M. N. R. Ashfold, *J. Chem. Soc., Faraday Trans.*, 1997, **93**, 3757.
31 M. W. Chase, Jr., C. A. Davies, J. R. Downey, Jr., D. J. Frurip, R. A. McDonald and A. N. Syverud, *J. Phys. Chem. Ref. Data*, 1985, **14**, suppl. 1.
32 T. J. Buckley, R. D. Johnson III, R. E. Huie, Z. Zhang, S. C. Kuo and R. B. Klemm, *J. Phys. Chem.*, 1995, **99**, 4879 and references therein.
33 V. D. Knyazev, A. Benczura and I. R. Slagle, *J. Phys. Chem. A*, 1997, **101**, 849.
34 M. R. Zachariah, P. R. Westmoreland, D. R. Burgess, Jr., W. Tsang and C. F. Melius, *J. Phys. Chem. A*, 1996, **100**, 8737.
35 D. A. Dixon and D. Feller, *J. Phys. Chem. A*, 1998, **102**, 8209.
36 R. Becerra, I. W. Carpenter and R. Walsh, *J. Phys. Chem. A*, 1997, **101**, 4185.
37 M-C. Chuang, M. F. Foltz and C. B. Moore, *J. Chem. Phys.*, 1987, **87**, 3855.
38 Th. Krossner, L. Zülicke, R. Vetter, M. Peric and S. D. Peyerimhoff, *J. Chem. Phys.*, 1994, **101**, 3973.
39 Th. Krossner, M. Peric, R. Vetter and S. D. Peyerimhoff, *J. Chem. Phys.*, 1994, **101**, 3981.

Paper 8/09693G